Applied Catalysis B: Environmental 89 (2009) 223–228

Contents lists available at ScienceDirect

Applied Catalysis B: Environmental

journal homepage: www.elsevier.com/locate/apcatb

High surface area tungsten carbide microspheres as effective Pt catalyst support for oxygen reduction reaction

Yi Wang [a], Shuqin Song [a], Vasiliki Maragou [b], Pei Kang Shen [a,**], Panagiotis Tsiakaras [b,*]

[a] State Key Laboratory of Optoelectronic Materials and Technologies, School of Physics and Engineering, Sun Yat-Sen University, Guangzhou 510275, China
[b] Department of Mechanical Engineering, School of Engineering, University of Thessaly, Pedion Areos 38334, Volos, Greece

ARTICLE INFO

Article history:
Received 30 July 2008
Received in revised form 14 November 2008
Accepted 22 November 2008
Available online 6 December 2008

Keywords:
Tungsten carbides
Proton exchange membrane fuel cells
Oxygen reduction reaction

ABSTRACT

In the present work, the preparation of high surface area (256 $m^2 g^{-1}$) tungsten carbide microspheres (TCMSs) by the aid of a simple hydrothermal method is realized and the performance of the Pt electrocatalyst supported on the as-prepared TCMSs towards the oxygen reduction reaction (ORR) is investigated. The SEM micrographs indicated that both the synthesized carbon microspheres (CMSs) and TCMSs showed perfect microsphere structure and uniform size. The EDX measurements confirmed that when the C/W mass ratio is ~2.5/1, tungsten and carbon coexist in the microspheres. Moreover, from the XRD results, it can be found that both W_2C and WC are detected and W_2C exists as the main phase. It was found that the Pt particles are uniformly dispersed on the supports, while the corresponding average particle size is ~3.7, 4.1 and 4.3 nm for Pt/C, Pt/CMSs and Pt/TCMSs, respectively. It was also found that in terms of ORR onset potential and mass activity, the Pt/TCMSs catalyst exhibits superior performance to that of Pt/CMSs and Pt/C, enhancing the ORR catalytic activity by more than 200%. The above behavior could be attributed to its higher electrochemical surface area (ESA), as well as to the synergistic effect between Pt and tungsten carbides.

1. Introduction

The most widely used cathode catalyst in proton exchange membrane fuel cells (PEMFCs) is nano-structured Pt particles dispersed on carbon materials. However, due to the sluggish process of oxygen reduction reaction (ORR), its corresponding overpotential is more than 0.2 V, even under open circuit conditions [1]. Recently, many efforts have been oriented towards the development of new ORR electrocatalysts, either with lower Pt loading or non-Pt electrocatalysts [2–6], focusing also on the synergistic effect between catalyst and support [7–9]. Tungsten carbide has been intensively studied since Levy and Boudart discovered that it possesses catalytic properties similar to those of platinum group metals [10]. In electrocatalysis, tungsten carbides have been mainly used as the electrocatalyst supports for methanol oxidation [11–13], oxygen reduction [7,14], nitrophenol oxidation [15,16] and hydrogen evolution [17,18]. Although the stability of tungsten carbides is still controversial [11,19–21], they are highly tolerant to both carbon monoxide and bisulfide [22,23]. However, the low surface area of tungsten carbides limits their application as the support materials in the electrocatalysts for PEMFCs and the related fields. In the present work, the preparation of high surface area tungsten carbide microspheres (TCMSs) by the aid of a simple hydrothermal method is realized and the performance of the Pt electrocatalyst supported on the as-prepared TCMSs towards oxygen reduction reaction is investigated. The corresponding structural characteristics were determined by the techniques of X-ray diffraction (XRD), scanning electron microscopy (SEM), transmission electron microscopy (TEM), energy dispersive X-ray spectroscopy (EDX) and Brunauer–Emmet–Teller (BET) method. Finally, the activity towards the oxygen reduction reaction was investigated with the electrochemical methods of cyclic voltammetry (CV), rotating disk electrode (RDE) voltammetry and electrochemical impedance spectroscopy (EIS).

2. Experimental

2.1. Preparation of the materials

The high surface area TCMSs were synthesized by using a simple hydrothermal method. The desired quantity of glucose and ammonium metatungstate (AMT) salt was dissolved in de-ionized water to form a transparent solution. The glucose/AMT molar ratio was kept equal to 100:1. The solution was then heated up to 170 °C at a rate of 5 °C min^{-1} and kept for 12 h in a sealed 50 ml Teflon-lined stainless autoclave. After left to be cooled down to the room

* Corresponding author. Tel.: +30 24210 74065; fax: +30 24210 74050.
** Co-corresponding author. Tel.: +86 20 84036736; fax: +86 20 84113369.
E-mail addresses: stsspk@mail.sysu.edu.cn (P.K. Shen), tsiak@mie.uth.gr (P. Tsiakaras).

0926-3373/$ – see front matter © 2008 Elsevier B.V. All rights reserved.
doi:10.1016/j.apcatb.2008.11.032

temperature, the product was filtered, washed by de-ionized water and ethanol in sequence several times, and finally dried in a vacuum oven at 70 °C for 6 h. In order to form tungsten carbides, the as-prepared product was heated up to 950 °C at a rate of 4 °C min^{-1}, in the presence of high purity argon flow in a quartz tube, and then carbonized at 950 °C in argon atmosphere for 2 h. Finally, it was further treated at the same temperature in the presence of hydrogen flow for 1 h, in order to remove the free carbon from TCMSs' surface [24].

A tentative mechanism of TCMSs' formation involves two steps, as schematically displayed in Fig. 1. In the first step, the organic glucose and tungsten-containing AMT formed a complex mixture of microspheres under hydrothermal conditions [25]. In the second step, the high-temperature treatment is for the further carbonization and then the TCMSs formation. The carbon microspheres (CMSs) were synthesized by following the exactly same procedure, without the addition of AMT.

The Pt/TCMSs catalysts were prepared by the intermittent microwave heating (IMH) method, as previously described [26,27]. Chloroplatinic acid was well mixed in a beaker with ethylene glycol (EG) by stirring in an ultrasonic bath. Thereafter, TCMSs were added into the mixture as the support. As soon as the pH value of the system was adjusted above 10, by the drop-wise addition of 2.0 mol dm^{-3} NaOH/EG solution, a well-dispersed slurry was obtained after stirring in an ultrasonic bath for 30 min. Finally, the slurry was microwave-heated in the pulse form of every 10 s for several times and the resulting black solid sample was filtered, washed and dried at 80 °C in a vacuum oven for 10 h. For comparison, Pt supported on XC-72 C and the as-prepared CMSs were also prepared by following the same procedure as above.

2.2. Characterization

The X-ray diffraction measurements were carried out by the aid of a D/Max-IIIA (Rigaku Co., Japan) employing Cu K_α (λ = 0.15406 nm) as the radiation source at 40 kV and 40 mA. The transmission electron microscopy investigations were performed on a JEOL JEM-2010 (HR) operating at 200 kV. The morphology of the samples was obtained by scanning electron microscopy (LEO-1530VP, Germany). The energy dispersive X-ray spectroscopy technique was used for the elemental characterization. The Brunauer–Emmett–Teller surface area was measured by an automatic volumetric sorption analyzer (Quantachrome, Nova1200).

All the electrochemical measurements were conducted on a PARSTAT 2273 instrument in a three-electrode cell at room temperature, with a saturated calomel electrode (SCE) as the reference electrode and a platinum foil as the counter electrode, respectively. The working electrode was prepared with the glass carbon rotating disk as the substrate. Its diameter was 0.5 cm. Typically, a mixture containing 5.0 mg electrocatalyst, 0.9 ml ethanol and 0.1 ml Nafion solution (5 wt%, DuPont, USA) was ultrasonicated for 15 min to obtain a well-dispersed ink. The catalyst ink was then quantitatively transferred onto the surface of the glass carbon electrode and dried under infrared lamp to obtain a catalyst thin film. The catalyst loading was 0.25 mg cm^{-2}. The electrochemical tests were performed in nitrogen or oxygen saturated 0.5 mol dm^{-3} H_2SO_4 aqueous solution at room temperature. The electrochemical impedance spectra (EIS) were collected at 0.75 V in the O_2-saturated 0.5 mol dm^{-3} H_2SO_4 in a frequency range from 10 kHz to 0.1 Hz with 10 points per decade. The amplitude of the AC-voltage was 5 mV. Without specification, the potential in the present paper was referred to normal hydrogen electrode (NHE).

3. Results and discussion

From the SEM micrographs given in Fig. 2a and b, it can be clearly seen that both the as-synthesized carbon microspheres and tungsten carbide microspheres present perfect microsphere structure and uniform size. The average diameter of the CMSs is approximately 0.5 μm (Fig. 2a). However, based on the SEM and TEM results (Fig. 2b and c), one can distinguish that the corresponding diameter of TCMSs is obviously bigger (*ca.* 1.2 μm) than that of CMSs. The size increment of TCMSs could be attributed at least to the following two reasons: (i) the addition of AMT could play a catalysis role in the hydrothermal carbonization of glucose during the hydrothermal process; (ii) AMT can affect the stability of the intermediate colloid products formed under hydrothermal conditions, as previously reported by Thomas and co-workers [28]. From the EDX results shown in the inset of Fig. 2b, it can be confirmed that when the C/W mass ratio is ~2.5/1, tungsten and carbon coexist in the microspheres. As known, the sphere structure of the micrometer size TCMSs favors the mass transfer. This becomes especially important when employed as the catalyst support materials in liquid environment, like in the case of direct alcohol fuel cells (DAFCs) and electrochemical sensors, due to the fact that the mass transfer becomes a challenge in the liquid case.

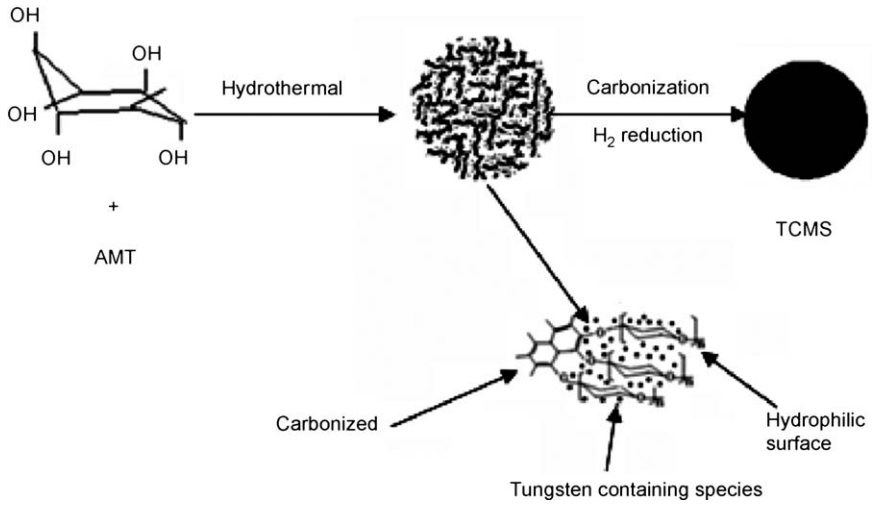

Fig. 1. Schematic model for the formation of tungsten carbide microspheres.

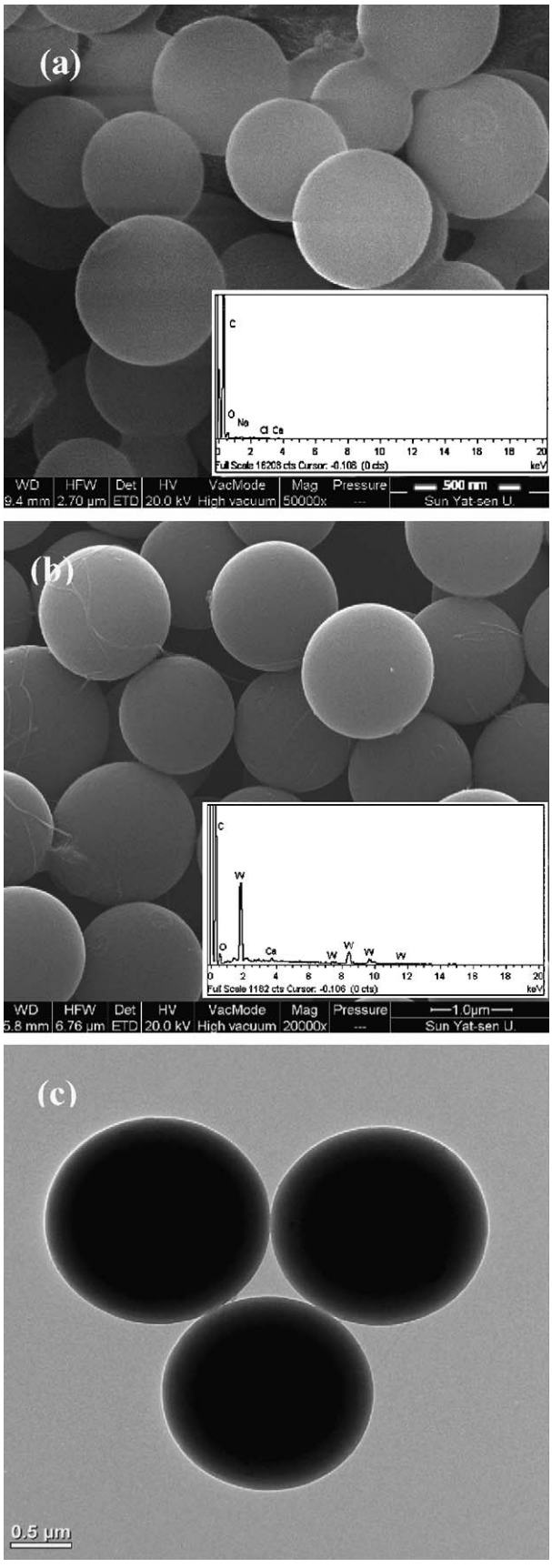

Fig. 2. The SEM micrographs of (a) CMSs and (b) TCMSs and (c) TEM image of TCMSs. The insets in (a) and (b) are the EDX patterns of CMSs and TCMSs, respectively.

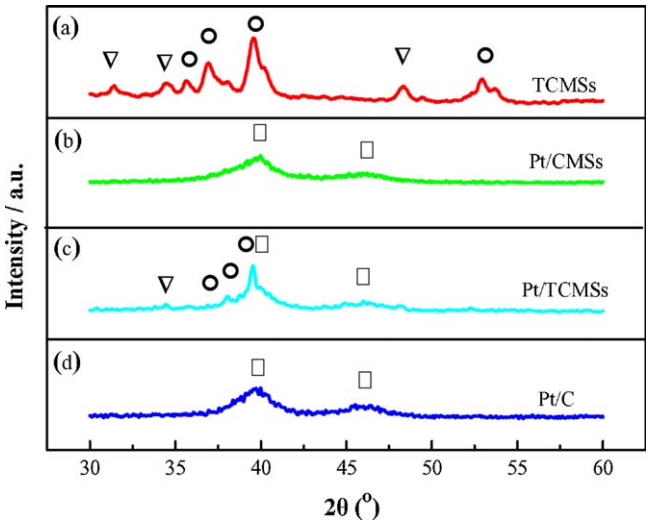

Fig. 3. The XRD patterns of samples (a) TCMSs, (b) Pt/CMSs, (c) Pt/TCMSs and (d) Pt/C. (○) W_2C, (▽) WC and (□) Pt.

Fig. 3a shows the typical XRD patterns of the TCMSs. The respective diffraction peaks at 31.44°, 35.02°, 48.35° correspond to (0 0 1), (1 0 0) and (1 0 1) facets of WC, while those at 2θ of 35.5°, 36.9°, 40.1°, 52.8° correspond to (2 0 0), (1 2 1), (1 0 2) and (2 2 1) facets of W_2C, respectively. These results indicate that the TCMSs obtained by following the proposed preparation procedure, as presented in Fig. 1, are a mixture of WC and W_2C. Additionally, it is worth mentioning that from the experimental results it has been concluded that the ratio of WC to W_2C in the mixture depends on the initial molar ratio of ammonium metatungstate to glucose at the same carbonation temperature and time. Furthermore, the content of the WC phase increases along with the increase of AMT content in the original solution, which is in agreement with already reported results by Ganesan and Lee [11]. For the sake of comparison, the Pt/CMSs (20 wt% Pt), Pt/TCMSs (10 wt% Pt) and Pt/C (20 wt% Pt) electrocatalysts were prepared and their corresponding XRD results are presented in Fig. 3b–d, respectively. The diffraction peaks at 39.8° and 46.7° correspond to the (1 1 1) and (2 0 0) crystalline planes of fcc Pt. Indeed, the broaden peak centered at 39.2° is the overlapped peak of the (1 1 1) peak of Pt and the (1 0 2) peak of W_2C.

Fig. 4 shows the N_2 adsorption/desorption isothermal curves for TCMSs, while in the inset of Fig. 4 the corresponding pore size distribution and pore volume of TCMSs are presented. A quasi IV isotherm can be distinguished, characterized by a hysteretic loop at the relative pressure P/P_0 ranging from 0.5 to 0.8. The measured BET specific surface area of TCMSs is 256 $m^2\ g^{-1}$. The surface areas of the commercial WC products and those synthesized by other methods are only several to some dozens of $m^2\ g^{-1}$ [16,29,30]. The further analysis of the BET data based on the Horvath–Kawazoe (HK) and the Barrett–Joyner–Halenda (BJH) formulas reveals the presence of many micropores and some mesopores on the TCMSs' surface, which justifies the extremely high surface area. Due to their high surface area, TCMSs were adopted as the support of the Pt catalysts in the present work, while CMSs and XC-72 carbon powder (Cabot Co., USA) were in turn used as the supports for the sake of comparison.

Fig. 5 shows the TEM micrographs of Pt/CMSs (20 wt% Pt), Pt/TCMSs (10 wt% Pt) and Pt/C (20 wt% Pt). It can be distinguished that the Pt particles are uniformly dispersed on the supports, while the corresponding average particle size is approximately 4.1, 4.3 and 3.7 nm for Pt/CMSs, Pt/TCMSs and Pt/C, respectively. The elemental analysis results by the aid of EDX are given in the insets of the

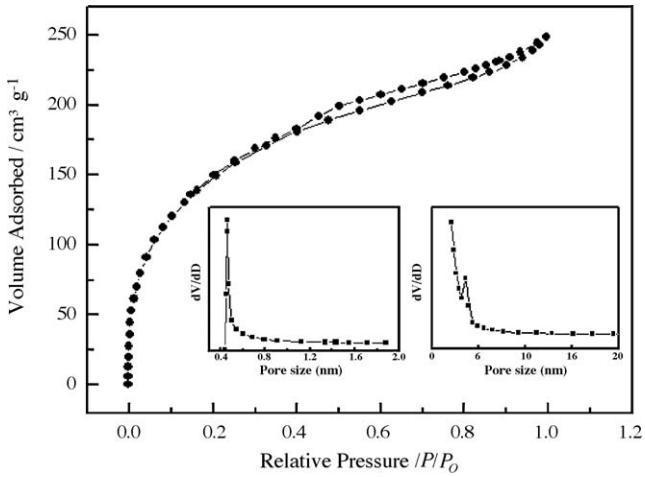

Fig. 4. The nitrogen adsorption/desorption isothermal curves of TCMSs. The insets show the corresponding pore size distribution and pore volume of TCMSs.

corresponding figures. The EDX results of Pt/TCMSs (10 wt% Pt) (Fig. 5b) indicate the co-existence of Pt, W and C in the specific sample.

In order to investigate the electrocatalytic performance of the as-prepared electrocatalysts for the oxygen reduction reaction, RDE experiments with different catalysts in an O_2-saturated 0.5 mol dm^{-3} H_2SO_4 aqueous solution were carried out at room temperature. The curves were obtained with a potential scan rate of 5 mV s^{-1} at 2500 rpm and the corresponding results are shown in Fig. 6. It can be seen that the pure TCMSs are inactive towards ORR, while the other three catalysts exhibit significant catalytic activity. At this point, it should be noted that in the case of pure TCMSs used, curve 1 just shows the performance and there is no relationship with the units of *y*-axis. By comparing the corresponding ORR performance of these three Pt-based catalysts, one can conclude that Pt/TCMSs exhibits superior ORR specific mass activity and specific activity to those of Pt/CMSs and Pt/C. For further comparison, Table 1 summarizes the electrochemical data of ORR over the different catalysts used. It is clear that the onset potential of ORR on Pt/TCMSs (0.95 V *vs*. NHE) is higher than that on Pt/C catalyst (0.88 V *vs*. NHE), indicating that the introduction of TCMSs to the Pt catalyst strongly improves its ORR activity. The positive shift of about 70 mV for the ORR onset potential is significant, since the reasonable voltage output for a single H_2/O_2 fuel cell is around 0.6–0.7 V. For the Pt/TCMSs catalyst, the current values per gram of Pt at 0.80 V (*vs*. NHE) are approximately more than twofold higher than that of the other two catalysts. This can be attributed to the higher electrochemical surface area (ESA) of the Pt/TCMSs catalyst obtained from the CV results recorded in 0.5 mol dm^{-3} H_2SO_4 solution, as shown in Table 1, as well as to the synergistic effect between Pt and tungsten carbides [6,14]. With half of the Pt loading, Pt/TCMSs still gives comparable or even better performance than Pt/C. It is quite important to reduce the Pt usage and consequently to decrease the cost of the catalysts and fuel cells.

Table 1
Comparison of the catalytic activities of various catalysts for the reaction of oxygen reduction.

Catalysts	Onset potential/V	Mass activity@ 0.8 V/A g^{-1} Pt	ESA/m^2 g^{-1} Pt	Specific activity@ 0.8 V/μA cm^{-2} Pt
Pt/C	0.88	18.5	37.2	49.7
Pt/CMSs	0.85	17.0	23.8	71.4
Pt/TCMSs	0.95	41.7	53.7	77.6

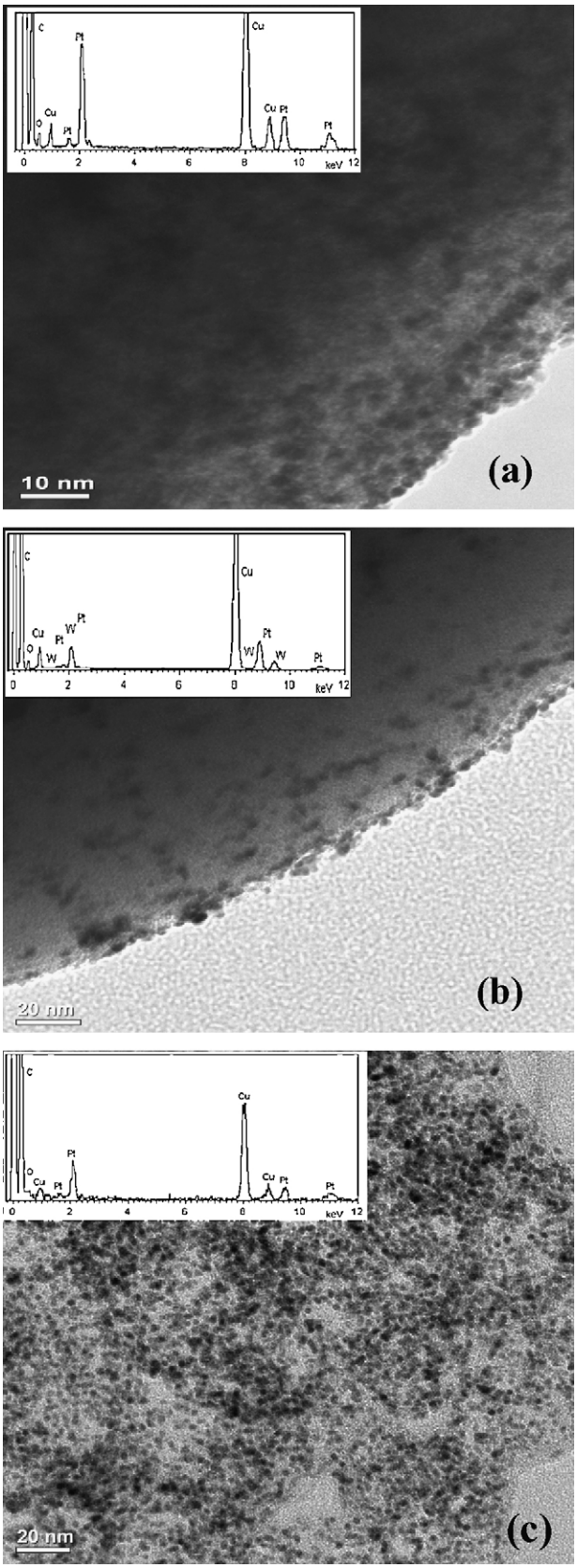

Fig. 5. The TEM images of (a) 20 wt% Pt/CMSs, (b) 10 wt% Pt/TCMSs and (c) 20 wt% Pt/C. The insets show the corresponding EDX patterns.

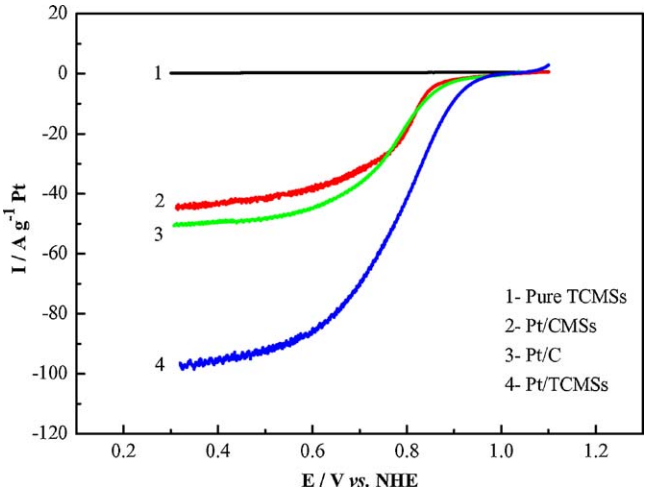

Fig. 6. Linear potential sweep curves of ORR on different electrocatalysts in an O_2-saturated 0.5 mol dm^{-3} H_2SO_4 aqueous solution at 2500 rpm and a potential scan rate of 5 mV s^{-1}.

For the further evaluation of the ORR mechanism on Pt/TCMSs, the polarization curves were recorded at different rotating rates on the rotating disk electrode coated with Pt/TCMSs catalyst in an O_2-saturated 0.5 mol dm^{-3} H_2SO_4 aqueous solution at room temperature (Fig. 7). It is obvious that the catalytic current increases along with the increase of the electrode rotating rate. Higher current values at higher rotating rates indicate a higher catalyst turnover rate for the ORR at the electrode. For the further kinetic analysis of the ORR process over the thin film electrode, the reciprocal of the observed currents at 0.75 V from Fig. 7a were plotted against the reciprocal of the square root of rotating rates, as shown in Fig. 7b, according to the Koutecký–Levich equation as follows [31,32]:

$$\frac{1}{I} = \frac{1}{I_k} + \frac{1}{B\omega^{1/2}} \quad (1)$$

where I represents the experimentally measured current, I_k the kinetic current, $B = 0.62nFAC_{O_2}(D_{O_2})^{2/3}\nu^{-1/6}$, ω the rotating rate in rad s^{-1}, n the electrons number involved, F the Faraday's constant, A the electrode area, C_{O_2} the bulk concentration of O_2, D_{O_2} the diffusion coefficient of O_2 and ν the kinematic viscosity of the electrolyte. It can be found that the linear curve obtained experimentally is strictly parallel to the theoretical line of the four-electron reduction mechanism, indicating a four-electron pathway for the ORR on Pt/TCMSs catalyst.

The chronoamperometric measurements of the ORR over Pt/TCMSs, Pt/CMSs and Pt/C catalysts at 0.75 V (*vs.* NHE) show that the steady-state current density for the ORR on Pt/TCMSs is more than 200% higher compared to the other two catalysts (Fig. 8). This is in agreement with the RDE results as given in Fig. 6. Finally, the electrochemical impedance spectroscopy measurements were carried out on all of the as-prepared catalysts at 0.75 V (*vs.* NHE) and the results are shown in Fig. 9. The charge transfer resistance R_{ct}, as measured by the diameter of the semicircle in the plot, is related to the charge transfer reaction kinetics according to the following Eq. [33,34]:

$$R_{ct} = \frac{RT}{nFi_0} \quad (2)$$

where

$$i_0 = nFAk_0 C_O^{*(1-\alpha)} C_R^{*\alpha} \quad (3)$$

R is the molar gas constant (J mol^{-1} K^{-1}); T is the temperature (K); n is the number of electrons transferred; F is the Faraday constant

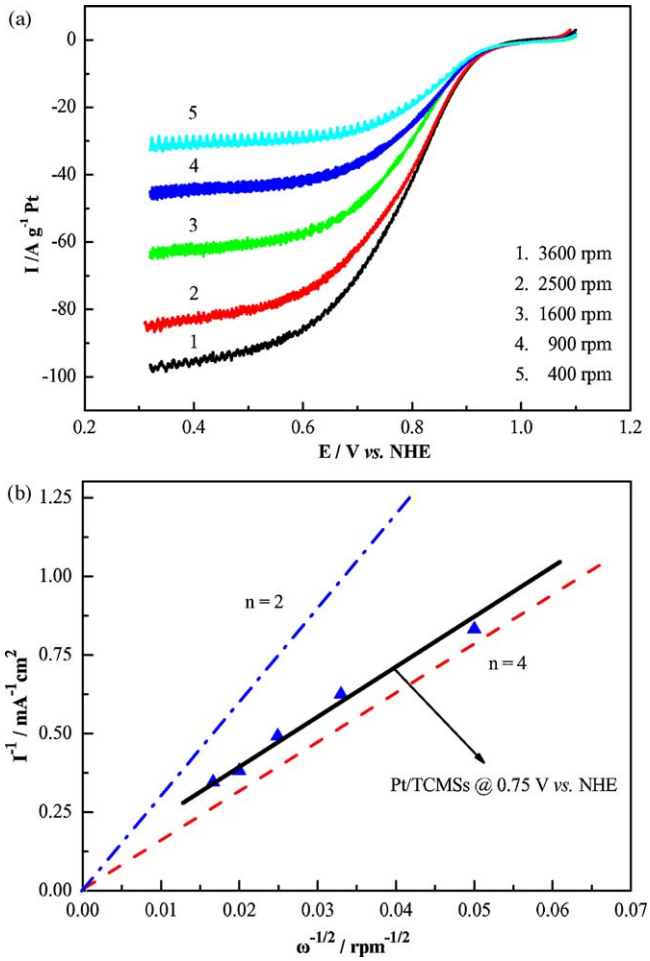

Fig. 7. (a) The ORR polarization curves over Pt/TCMSs catalyst at different rotating rates in an O_2-saturated 0.5 mol dm^{-3} H_2SO_4 aqueous solution at room temperature and (b) the corresponding Koutecký–Levich plots. The dashed lines are plotted based on the theoretical calculation according to the Koutecký–Levich equation for two- and four-electron O_2 reduction processes.

(C); i_0 is the exchange current (A); A is the reaction area (cm^2); k_0 is the standard heterogeneous rate constant (cm s^{-1}); C_O^*, C_R^* are the respective bulk concentration of oxidation and reduction species (mol L^{-1}); and α is the transfer coefficient. Considering that the

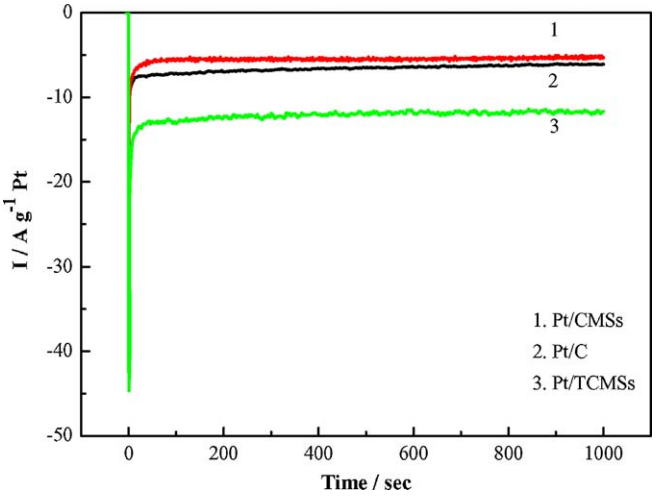

Fig. 8. The chronoamperometric curves of the ORR on Pt/TCMSs, Pt/CMSs and Pt/C electrocatalysts in an O_2-saturated 0.5 mol dm^{-3} H_2SO_4 aqueous solution at 0.75 V (*vs.* NHE).

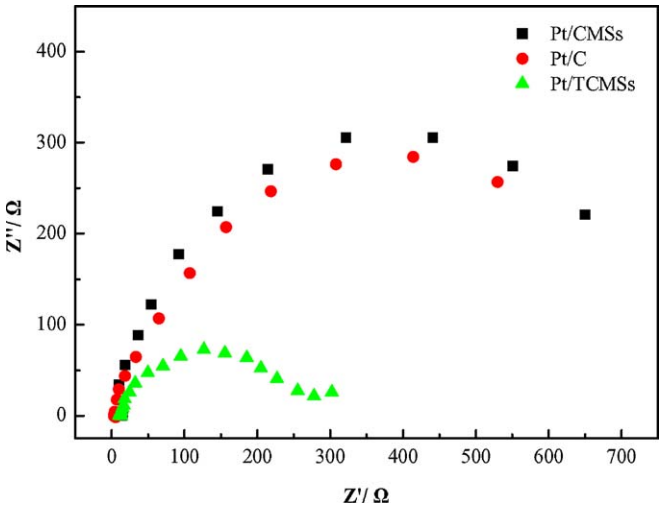

Fig. 9. Nyquist plots of EIS for ORR on Pt/TCMSs, Pt/CMSs and Pt/C catalysts in an O_2-saturated 0.5 mol dm^{-3} H_2SO_4 aqueous solution at 0.75 V (*vs.* NHE). The frequencies range from 10 kHz to 0.1 Hz.

semicircle in EIS curves represents the ORR charge transfer resistance (R_{ct}), it can be clearly seen from Fig. 9 that the corresponding R_{ct} in the case of Pt/TCMSs is the smallest among the three catalysts at the investigated potential. This indicates that the ORR on Pt/TCMSs catalyst is more favorable compared to the other two catalysts, due to the enhanced reaction kinetics [35], which is in good agreement with the above results.

4. Conclusions

In the present work, tungsten carbide microspheres with uniform particle size and high surface area (256 m^2 g^{-1}) were synthesized by using a simple hydrothermal method for the first time. The Pt nanoparticles were uniformly distributed on these support materials through the intermittent microwave heating method. The as-prepared Pt/TCMSs catalyst in terms of oxygen reduction reaction onset potential and mass activity exhibits superior performance to that of Pt/CMSs and Pt/C catalysts. The enhanced performance of Pt/TCMSs for the oxygen reduction reaction could be attributed to its higher electrochemical surface area, as well as to the synergistic effect between Pt and tungsten carbides. The sphere structure of the TCMSs in micrometer size as catalyst support is favorable for the mass transfer and the formation of three-phase interface increasing consequently the active surface area. For all the above-mentioned characteristics, TMCSs can be potentially used in liquid environment, like in the case of direct alcohol fuel cells and electrochemical sensors.

Acknowledgements

This work was supported by the Guangdong Science and Technology Key Projects (2007A010700001, 2007B090400032), Guangzhou Science and Technology Key Project (2007Z1-D0051) and the Scientific Research Foundation for Young Teachers of Sun Yat-Sen University.

References

[1] S. Arico, S. Srinivasan, V. Antonucci, Fuel Cells 1 (2001) 133–161.
[2] M.H. Shao, K. Sasaki, R.R. Adzic, J. Am. Chem. Soc. 128 (2006) 3526–3527.
[3] J.L. Fernandez, V. Raghuveer, A. Manthiram, A.J. Bard, J. Am. Chem. Soc. 127 (2006) 13100–13101.
[4] L. Zhang, J.J. Zhang, D.P. Wilkinson, H.J. Wang, J. Power Sources 156 (2006) 171–177.
[5] V. Raghuveer, P.J. Ferreira, A. Manthiram, Electrochem. Commun. 8 (2006) 807–814.
[6] S. Song, Y. Wang, P. Tsiakaras, P.K. Shen, Appl. Catal. B 78 (2008) 381–387.
[7] H. Meng, P.K. Shen, Chem. Commun. 1 (2005) 4408–4410.
[8] C.W. Xu, R. Zeng, P.K. Shen, Z.D. Wei, Electrochim. Acta 51 (2005) 1031–1035.
[9] M. Nie, H.L. Tang, Z.D. Wei, S.P. Jiang, P.K. Shen, Electrochem. Commun. 9 (2007) 2375–2379.
[10] R.L. Levy, M. Boudart, Science 181 (1973) 547–549.
[11] R. Ganesan, J.S. Lee, Angew. Chem. Int. Ed. 44 (2005) 6557–6560.
[12] D.R. McIntyre, G.T. Burstein, A. Vossen, J. Power Sources 107 (2002) 67–73.
[13] R. Ganesan, D.J. Ham, J.S. Lee, Electrochem. Commun. 9 (2007) 2576–2579.
[14] H. Meng, P.K. Shen, J. Phys. Chem. B 109 (2005) 22705–22709.
[15] G.H. Li, C.A. Ma, J.Y. Tang, J.F. Sheng, Electrochim. Acta 52 (2007) 2018–2023.
[16] G.H. Li, C.A. Ma, Y.F. Zheng, W.M. Zhang, Micropor. Mesopor. Mater. 85 (2005) 234–240.
[17] L. Schlapbach, A. Zuttel, Nature 414 (2001) 353–358.
[18] M. Wu, P.K. Shen, Z.D. Wei, S. Song, M. Nie, J. Power Sources 166 (2007) 310–316.
[19] S. Bodoardo, M. Maja, N. Penazzi, F.E.G. Henn, Electrochim. Acta 42 (1997) 2603–2609.
[20] C.J. Barnett, G.T. Burstein, A.R.J. Kucernak, K.R. Williams, Electrochim. Acta 42 (1997) 2381–2388.
[21] H. Chhina, S. Campbell, O. Kesler, J. Power Sources 164 (2007) 431–440.
[22] J.B. Christian, S.P.E. Smith, M.S. Whittingham, H.D. Abruna, Electrochem. Commun. 9 (2007) 2128–2132.
[23] M.K. Jeon, H. Daimon, K.R. Lee, A. Nakahara, S.I. Woo, Electrochem. Commun. 9 (2007) 2692–2695.
[24] F.H. Ribeiro, R.A.D. Boudart, Chem. Mater. 3 (1991) 805–812.
[25] X.M. Sun, Y.D. Li, Angew. Chem. Int. Ed. 43 (2004) 597–601.
[26] P.K. Shen, Z.Q. Tian, Electrochim. Acta 49 (2004) 3107–3111.
[27] S. Song, Y. Wang, P.K. Shen, J. Power Sources 17 (2007) 46–49.
[28] M.M. Titirici, M. Antonietti, A. Thomas, Chem. Mater. 18 (2006) 3808–3812.
[29] Y. Hara, N. Minami, H. Matsumoto, H. Itagaki, Appl. Catal. A 332 (2007) 289–296.
[30] G.H. Li, C.A. Ma, J.Y. Tang, Mater. Lett. 61 (2007) 991–993.
[31] L. Zhang, J. Zhang, D.P. Wilkinson, H. Wang, J. Electrochem. Soc. 152 (2005) A2421–A2426.
[32] H. Liu, L. Zhang, D. Ghosh, J. Jung, B.W. Downing, E. Whittemore, J. Power Sources 161 (2006) 743–752.
[33] S. Sen Gupta, S.S. Mahapatra, J. Datta, J. Power Sources 131 (2004) 169–174.
[34] A.J. Bard, L.R. Faulkner, Electrochemical Methods, Wiley, 1980.
[35] E.H. Yu, K. Scott, R.W. Reeve, J. Electroanal. Chem. 547 (2003) 17–24.